scientific reports

Check for updates

OPEN

Mesozoic larva in amber reveals the venom delivery system and the palaeobiology of an ancient lineage of venomous insects (Neuroptera)

Davide Badano[1,2]✉, Michela Fratini[3], Francesca Palermo[3], Nicola Pieroni[3], Laura Maugeri[3] & Pierfilippo Cerretti[4,5]

The larvae of Neuroptera are predators that feed by injecting bioactive compounds into their prey and then suctioning the fluids through modified mouthparts. We explore the evolutionary history of this feeding structure through the examination of a new fossil larva preserved in Late Cretaceous Kachin amber, which we describe as new genus and species, *Electroxipheus veneficus* gen et sp. nov. X-ray phase-contrast microtomography enabled us to study the anatomy of the larva in 3D, including the structure of the mouthparts and that of the venom delivery system. The specimen exhibited a unique combination of morphological traits not found in any known fossil or extant lacewing, including an unusual structure of the antenna. Phylogenetic analyses, incorporating a selection of living and fossil larval Neuroptera and enforcing maximum parsimony and Bayesian inference, identified the larva as belonging to the stem group Mantispoidea. The larva shows that the anatomy of the feeding and venom-delivery apparatus has remained unchanged in Neuroptera from the Cretaceous to the present. The morphology of the specimen suggests that it was an active predator, in contrast with the scarcely mobile, specialized relatives, like mantispids and berothids.

Keywords Cretaceous, Functional morphology, Holometabola, Neuropterida, Phylogeny, X-ray phase-contrast microtomography

During their long evolutionary history, insects evolved a diverse arsenal of biochemical weapons for both defence and attack. Envenomation, i.e., the injection of bioactive secretions altering animal behaviour and physiology, systems independently appeared in different insect lineages, each exhibiting unique adaptations[1,2]. Envenomation evolved in a diverse array of predatory insects feeding on animal fluids through paralytic compounds, including Heteroptera, Diptera and in the larvae of Neuroptera and of some Coleoptera[1,3]. Neuroptera, or lacewings, represent a relatively small (ca. 6000 described species) and ancient lineage of holometabolans dating back to the Permian[4,5]. Lacewing larvae are predators exhibiting a moderate diversity of morphologies and life histories, ranging from predators of small arthropods to sponge feedersor spider egg predators[6]. The predatory efficiency of lacewing larvae is also exploited in biocontrol, using green lacewings (Chrysopidae). Despite their diversity and morphological disparity, all lacewing larvae share a piercing and sucking apparatus formed by the highly modified mouthparts, which also serves as venom-delivery system (the only exception being Sisyridae)[7,8]. This piercing apparatus is composed of a ventrally grooved mandible that forms a suction channel by juxtaposition with the underlying dorsally grooved maxillary stylet. These two components maintain the function of the channel being held together by a seaming mechanism, consisting of a guide on the ventral side of the mandible and a prominent, apically folded, rail on the dorsal side of the maxillary stylet. The maxillary stylet is also provided with an internal lumen, or poison channel, which is ventrally coated at base with a layer of secretory cells, or maxillary gland[9–11]. These glands are likely the source of bioactive peptides acting as paralyzing venoms once

[1]Department of Life Science, University of Siena, 53100 Siena, Italy. [2]NBFC, National Biodiversity Future Center, Palermo, Italy. [3]Department of Physics, CNR-Nanotec (Rome Unit) c/o, Sapienza University of Rome, Rome, Italy. [4]Department of Biology and Biotechnologies "Charles Darwin", Sapienza University of Rome, Rome, Italy. [5]Museum of Zoology, Sapienza University of Rome, Rome, Italy. ✉email: davide.badano@unisi.it

injected through the poison channel into the prey[12]. Nevertheless, the chemical composition of the maxillary gland secretion, the transcription pathway, and the potential role of microbiota in venom production remain largely unknown[2].

Recent palaeontological progresses tremendously improved our knowledge of the past diversity of lacewings, especially at the larval stage, allowing to trace the evolution of anatomical and behavioral traits and their role in phylogenies. Cretaceous amber deposits document a phase of morphological experimentation among lacewings, improving our understanding of characters evolution and polarity during a period characterised by a peak in lacewing disparity[13–16]. The amber from Myanmar (Late Cretaceous from Kachin state, 98 ± 0.6 Ma[17]) represents a Rosetta stone to decipher the evolutionary history of lacewings, preserving an exceptional array of lacewing larvae, often distinguished by unusual morphologies[18–23]. Here we describe a new larval morphotype from Myanmar amber. The overall morphology of this specimen resembles the living larvae of the Mantispoidea, i.e., the clade of Neuroptera including Berothidae, Rhachiberothidae and Mantispidae[24], albeit lacking their main synapomorphies, making its phylogenetic affinities ambiguous. We investigated the morphology of this fossil through synchrotron X-ray phase-contrast microtomography (XPCT), allowing us to reconstruct the finest details of its anatomy in 3D and to unveil its phylogenetic affinities. XPCT is a nondestructive 3D imaging technique resulting in a better image contrast and spatial resolution by detecting transparent or weakly absorbing samples, due to its sensitivity to phase shifts. So, this technique increases the visibility of small structures undetectable in absorption mode[25].

XPCT is a cutting-edge technique for the study of fossil specimens, allowing to study anatomical features, such as bristles or wing details, of taxonomic importance but relatively small relative to the size of the whole organism[26].

The XPCT results allowed us to delve in the envenomation apparatus of a Mesozoic insect for the first time. Our findings suggest that i) functional features, such as the internal structure of the mouthparts, are highly conservative across the lacewing evolutionary history despite the high morphological disparity exhibited by fossils, and ii) stem group Mantispoidea were morphologically and ecologically diverse in the Mesozoic.

Results

Systematic Palaeontology

Neuroptera Linnaeus, 1758.

Mantispoidea Leach, 1815 (stem group).

Electroxipheus Badano & Cerretti gen. n.

Zoobank LSID urn:lsid:zoobank.org:act:EDA5E293-0A63-4879-96C9-EF64736BF90B

Etymology. The genus name is masculine, and it is a composite word from Greek, with prefix "electro", i.e. amber, and suffix "xipheus", i.e. swordsman, hence "amber swordsman" after the sword shaped jaws of the larva.

Diagnosis

Larva campodeiform, elongate (Fig. 1). Head capsule sclerotized, subrectangular, lacking lateral remnants of frontoclypeal sulcus. Ocular region with three stemmata. Frontal ecdysial suture present, lateral and coronal ecdysial sutures absent. Mandibulo-maxillary stylet largely straight, slightly curved outward apically and slightly bent downward in lateral view. Antenna thin, longer than stylet, with three antennomeres; second antennomere with three subsegments; third antennomere with one apical subsegment and lacking specialized terminal sensillum. Labium with trapezoidal submentum provided with a median triangular process and laterally subdivided in diverging cylindrical elements. Labial palp thin, as long as mouthparts, with three palpomeres of the second being the longest. Antenna and labial palpus smooth, without scale-like texture. Thorax not sclerotized. Legs well developed, tarsus with unguitractor processes and trumpet-shaped empodium. Abdomen composed of ten segments.

Type species. *Electroxipheus veneficus* sp. n.

Electoxipheus veneficus Badano & Cerretti sp. n.

(Fig. 1, 2, 3, 4, Supplementary Information Movie S1).

Zoobank LSID urn:lsid:zoobank.org:act:148F91A6-39F0-48C4-8FED-1DFEA43AE5CC

Holotype

MZURPAL00112 (Museum of Zoology, Sapienza University of Rome). One specimen preserved in an amber piece.

Etymology

The specific epithet "*veneficus*" is a Latin masculine name meaning "poisoner", after the well-preserved venom channel in the jaws.

Diagnosis.

As for the genus (vide supra).

Type locality and horizon

Northern Myanmar, Kachin Province, Hukawng Valley, c. 100 km west of the town of Myitkyina; Late Cretaceous (98 ± 0.6 Ma).

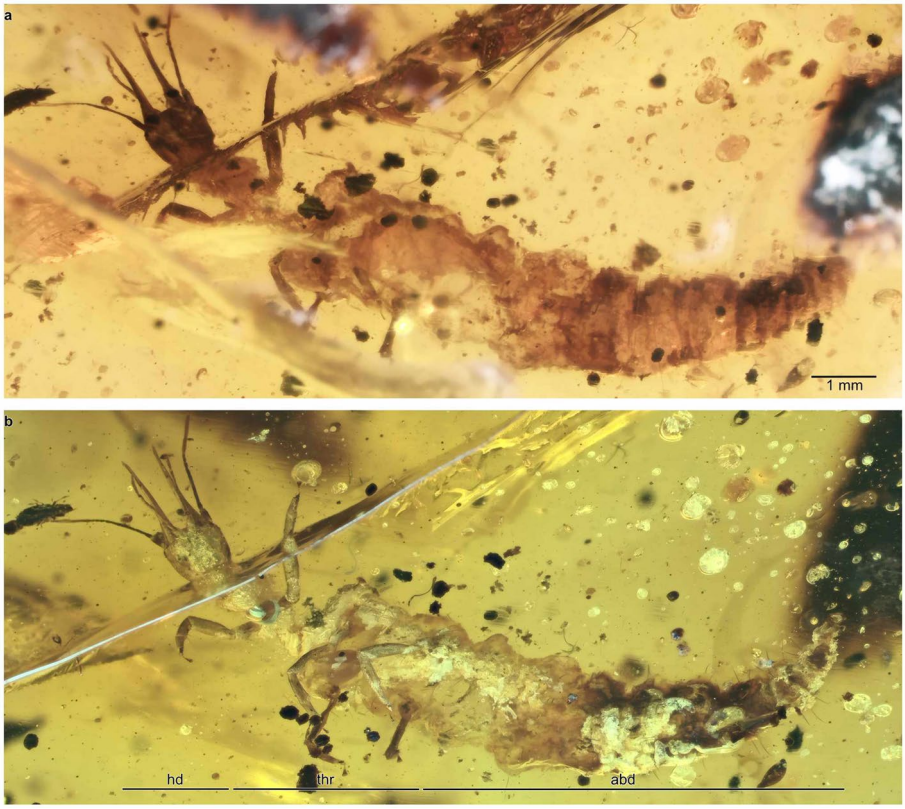

Figure 1. *Electroxipheus veneficus* gen. et sp. n., habitus. (**a**) dorsal view. (**b**) ventral view. hd, head; thr, thorax; abd, abdomen.

State of preservation

Specimen in good state of preservation, except for a fracture line crossing the cervical region and one prothoracic leg; thorax and anterior abdominal segments slightly damaged (Fig. 1).

Description

Second or third instar. *Measurements.* Head length: 0.9 mm; head width: 0.8 mm; jaws length: 1.36 mm; body length: 5.76 mm.

Head capsule

Head capsule subquadrate, as long as wide, tapering toward cervical region. Head sub rectangular in lateral view and largely flattened dorsally (Supplementary Information Movie S1). Head dorsally sclerotized and ventrally mostly occupied by maxillary parts (Figs. 2A, 3). Anterior labial margin straight, without prominences (Fig. 3A, B, D). Frontal ecdysial suture distinct, encasing half of head anterior width; arms of frontal sutures converging at head mid-length, curved toward each other (Fig. 3A). Lateral and coronal ecdysial sutures absent. Antenna inserted laterally, on short tubercle, posterior to mandibular-maxillary stylet (Fig. 3A). Ocular region posterior to antenna insertion, marked with dark pigments, with six small stemmata arranged in an upper and a lower row, each of three stemmata (Fig. 3A, C). Long hair-like sensillum rising between stemmata.

Antenna

Antenna longer than mouthparts, with three main antennomeres. Second and third antennomeres with subsegments at apex (Fig. 2A, B, C). Basal antennomere cylindrical, three times longer than wide. Second antennomere long and thin, its diameter half that of first antennomere, cylindrical and over ten times longer than wide, with three subsegments, of which the first longer than remainders (Fig. 2B). Third antennomere cylindrical, thin, much longer than wide with a short, apical fusiform subsegment. Apical subsegment with a short apical sensillum (Fig. 2C). Antenna cuticle without ornamentations.

Mandibular-maxillary complex: suction and poison channels

Mandible and maxilla tightly associated, forming a single functional unit shaped like a straight, stylet-like sucking apparatus (Fig. 3). Blade-like section of mandibular-maxillary complex longer than head capsule, much wider at base, progressively narrowing toward apex. Apical section of mandibular- maxillary complex slightly curved outward and slightly bent downward in lateral view (Fig. 3A, B, C). Mandible narrower at base and much thinner

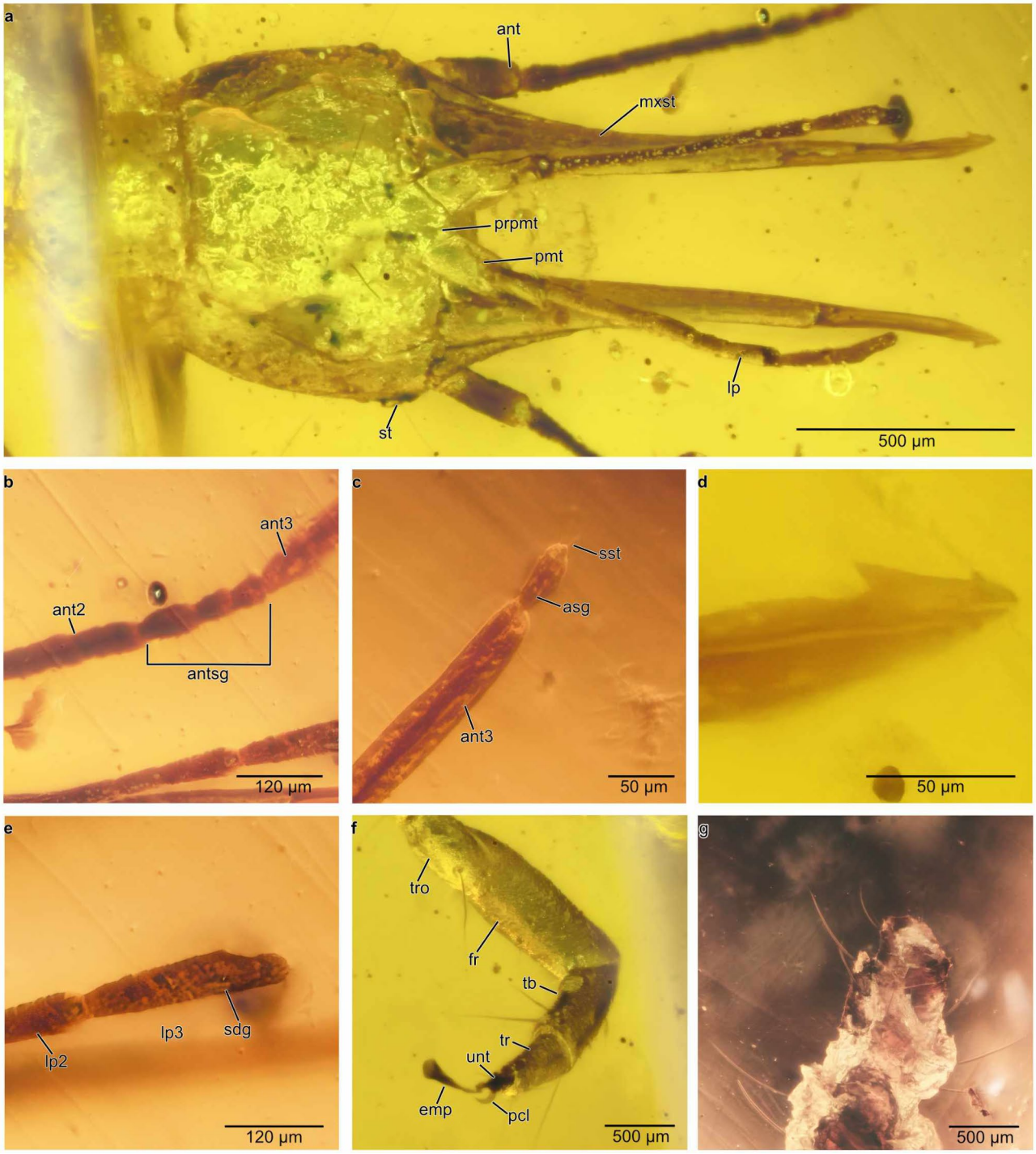

Figure 2. *Electroxipheus veneficus* gen. et sp. n., morphological details. (**a**) head capsule, ventral view. (**b**) antenna, subsegmentation of second antennomere. (**c**) tip of antenna and sensilla. (**d**) tip of mandibulo-maxillary stylet; (**e**) tip of labial palp and sensilla. (**f**) foreleg, ventral view. (**g**) abdomen tip. ant, antenna; ant 2, 2nd antennomere; ant3; 3rd antennomere; antsg, subsegments of 2nd antennomere; asg, apical subsegment; emp, empodium; fr, femur; lp, labial palp; lp2, 2nd palpomere; lp3; 3rd palpomere; mxst, maxillary stylet; pcl, pretarsal claw; prpmt, median process of prementum; pmt, prementum; sdg, digitiform sensillum; set, setae; sst, terminal sensillum; st, stemmata; tb, tibia; tr, tarsus; tro, trochanter; unt, unguitractor process.

than underlying maxilla, without teeth or serrations on internal margin. External margin of apex of mandible harpoon-shaped with a small inward tooth (Fig. 2D). Ventral surface of mandible concave, with a narrow groove running for almost its entire length, forming the roof of suction channel (Fig. 4). Suction channel externally

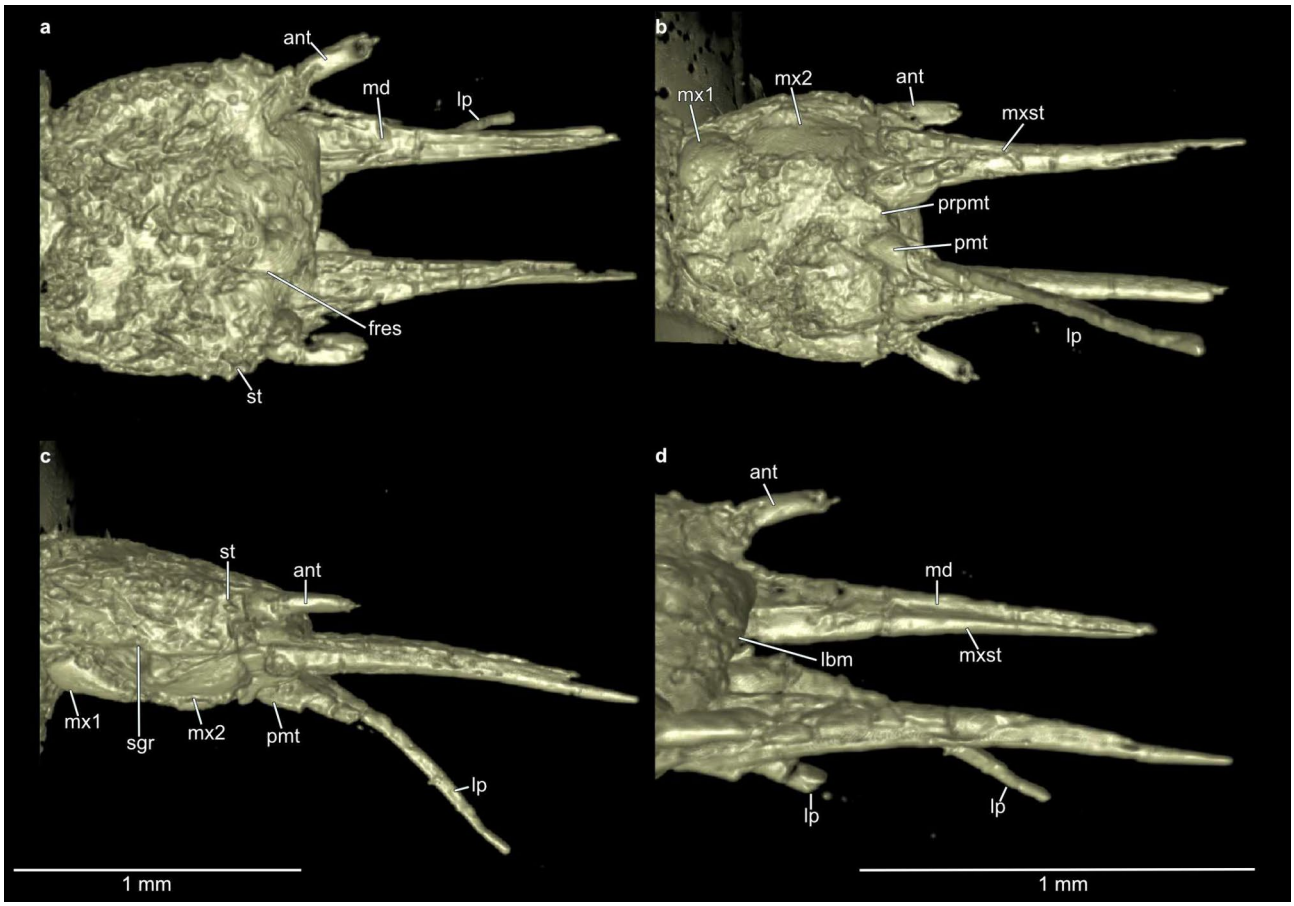

Figure 3. *Electroxipheus veneficus* gen. et sp. n., 3D rendering of XPCT image. (**a**) head, dorsal view; (**b**) head, ventral view; (**c**), head, lateral view; (**d**) mouthparts, dorso-lateral view. ant, antenna; fres, frontal ecdysial suture; lbm, labial margin; lp, labial palp; md, mandible; mx1, proximal maxillary element; mx2; distal maxillary element; mxst, maxillary stylet; prpmt, median process of prementum; pmt, prementum; sgr, subgenal ridge; st, stemmata.

delimited by a ridge, forming the protruding internal margin of a concave guide, in which fits the corresponding folded ridge on dorsal side of maxillary stylet (Fig. 4). Suction channel shifting dorsally in apical section of mandible, until it is almost delimited by mandible surface (Fig. 4). Maxilla inserted ventrally, partly retracted, divided in basal elements, and maxillary stylet. Apical and basal maxillary elements distinct, subdivided by a median furrow (Fig. 3B). Apical maxillary element longer than basal one, separated by ventrolateral margin of dorsal sclerotization of head by furrow (Fig. 3C). Blade-like section of maxilla robust, wider at base. Maxillary stylet similar in shape to mandible, but thicker. Dorsal side of maxillary stylet grooved, corresponding to ventral floor of suction channel (Fig. 4). Lateral side of suction channel groove closed by an apically folded guiding ridge, fitting in corresponding groove of mandible and interlocking mandible and maxilla (Fig. 4). Maxillary stylet with poison channel, which is progressively more superficial toward tip and opens just before apex of maxilla (Fig. 4).

Labium

Labium composed by a distinct mentum and submentum. Mentum scute-like, subrectangular, with a pair of trichoid sensilla. Submentum trapezoidal, with a prominent median triangular process, and subdivided in a pair of diverging cylindrical palpomere-like elements (Fig. 2A, 3B). Labial palp thin, as long as mandibulo-maxillary stylet, composed of three palpomeres. Basal palpomere widest, cylindrical; second palpomere longest element of palp; third palpomere gently swelling apically (Fig. 2A). Third palpomere with a digitiform sensillum near apex (Fig. 2E).

Thorax

Cervical area collar-like, largely membranous. Thorax largely membranous (Fig. 1). Prothorax preserving traces of paired dorsal sclerotizations. Prothorax longer and narrower than meso- and metathorax.

Legs

Legs cursorial, of similar shape (Fig. 1). Prothoracic leg more robust than following pairs. Prothoracic leg with coxa cylindrical; trochanter as long as 1/3 of femur, with a ventral trichoid sensillum; femur cylindrical, robust, three times longer than wide; tibia short, ventral side of femur with three trichoid sensilla at 2/3 of length; tarsus

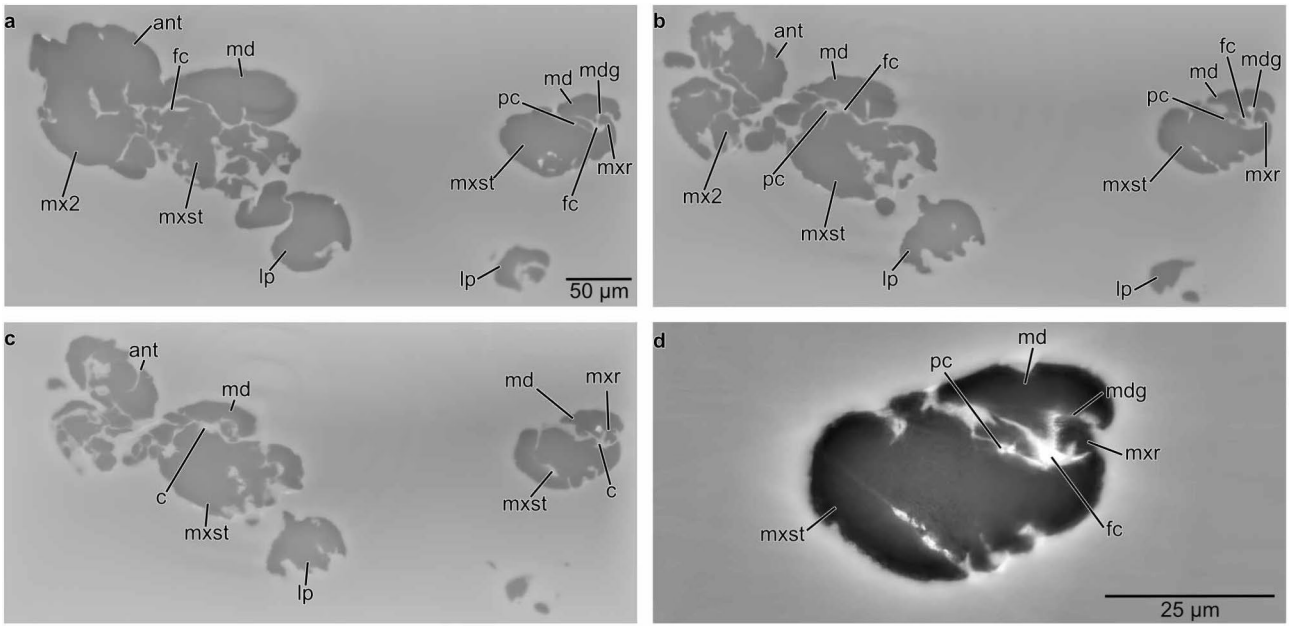

Figure 4. *Electroxipheus veneficus* gen. et sp. n., progressive cross sections (3 micron-thick slices in axial view) of mouthparts obtained with XPCT. (**a**); mandibulo-maxillary stylets, cross section at mid length; (**b**) mandibulo-maxillary stylets, cross section at two-thirds of length; (**c**) mandibulo-maxillary stylets, cross section at apex; (**d**) detail of cross section of one of the stylets. ant, antenna; c, channel; fc, food channel; lp, labial palp; md, mandible; mdg, mandible groove; mx2; distal maxillary element; mxr, maxillary ridge; mxst, maxillary stylet; pc, poison channel.

short, conical; pretarsus with a short unguitractor-process with a pair of curved claws and a well-developed, elongated trumpet- shaped empodium (Fig. 2F).

Abdomen

Abdomen composed of ten segments (Fig. 1). Abdominal segments decreasing in size posteriorly but otherwise of similar shape and structure. Sternites and tergites without sclerotizations. Pleurae with a median protuberance with one apical thin seta. Tergites and sternites with few short and thin setae, progressively increasing in size posteriorly. 9th abdominal segment longer than wide. 10th abdominal segment conical, with traces of pygopodium (Fig. 2G).

Morphological remarks

Electroxipheus exhibits a combination of character states shared with Mantispoidea (i.e., Berothidae, Rhachiberothidae, Mantispidae): i) lack of lateral remnants of the frontoclypeal sulcus, ii) straight mandibulo-maxillary stylets, iii) presence of an unguitractor process on tarsus[8,27–29]. *Electroxipheus* additionally exhibits a prominent median process on the prementum, a feature it shares with Berothidae. Coniopterygidae evolved a superficially similar labial process, although the broadly different anatomy of the labium in these clades suggests that they are not homologous. This structure is instead absent in Mantispidae[29]. In *Electroxipheus*, the process of prementum is more prominent than in extant berothids and divides the prementum in two distinct cylindrical elements, widely diverging at base and resembling palpomeres in shape. Conversely, in extant berothids, the labial palps are in close contact and contiguous at the base[29]. The condition observed in *Electroxipheus* resembles the organization of the prementum of the larvae of Myrmeleontoidea, in which the premental elements are widely separated and appear as palpomere-like[29,30]. Despite the fossil larva shares with Mantispoidea most diagnostic characters, it lacks their apomorphies, i.e., the scale-like texture of the antennae and mouthparts, and the sensilla inserted in deep alveoli[28,29,31]. Moreover, the head of *Electroxipheus* is wider than long, a marked difference from most mantispoids in which the head is much longer than wide at least in the first instar larva, except for Mantispidae Mantispinae . *Electroxipheus* also differs from Berothidae lacking the lateral sutures of head capsule. Most living mantispoid larvae are characterised by the reduction in the number of stemmata, which can be completely lost[32]. However, *Electroxipheus* is equipped with six stemmata, as observed in other fossil mantispoid larvae and in the larva of the living *Mucroberotha* Tjeder[31,33,34]. *Electroxipheus* also lacks a specialized terminal sensillum at the tip of the antenna, a character found in all mantispoids and several other clades of lacewings[29].

Phylogenetic analysis

The Maximum parsimony (MP) analysis under equal weights yielded 936 most-parsimonious trees (tree length = 368 steps; consistency index = 0.535; retention index = 0.854). The strict consensus cladogram is shown in Supplementary Information Fig. S1. When enforcing implied weights, the analyses generated different topologies

according to the selected k-value of the default weighting function. The topology derived from the best-fitting k-value (k = 10.239) obtained by the "setk.run" algorithm was selected for discussing the relationships within Neuroptera and for reconstructing the affinities of the fossil larva and mapping the evolution of character states (Fig. 5, Supplementary Information Fig. S2). Under these conditions, the search yielded 2 most-parsimonious trees with a tree length of 370 steps and a total fit of 12.596.

The performed phylogenetic analyses differ in the reconstruction of the phylogenetic backbone of Neuroptera and in the resolution of some clades, although they were broadly consistent in recovering the affinities of *Electroxipheus* (Figs. 5, 6, Supplementary Information Figs S1, S2). The MP analysis under implied weights (IW) resulted in the best resolved phylogeny, while the reconstructions under both MP enforcing equal weights (EW) and under Bayesian inference (BI) were largely unresolved. The monophyly of Neuroptera was strongly supported in all analyses (MP Bremer support: 6; BI Posterior Probability: 100). Under IW, Coniopterygidae emerged as the sister group to all remaining Neuroptera based on one unique synapomorphy (84:1, cervical sclerite and

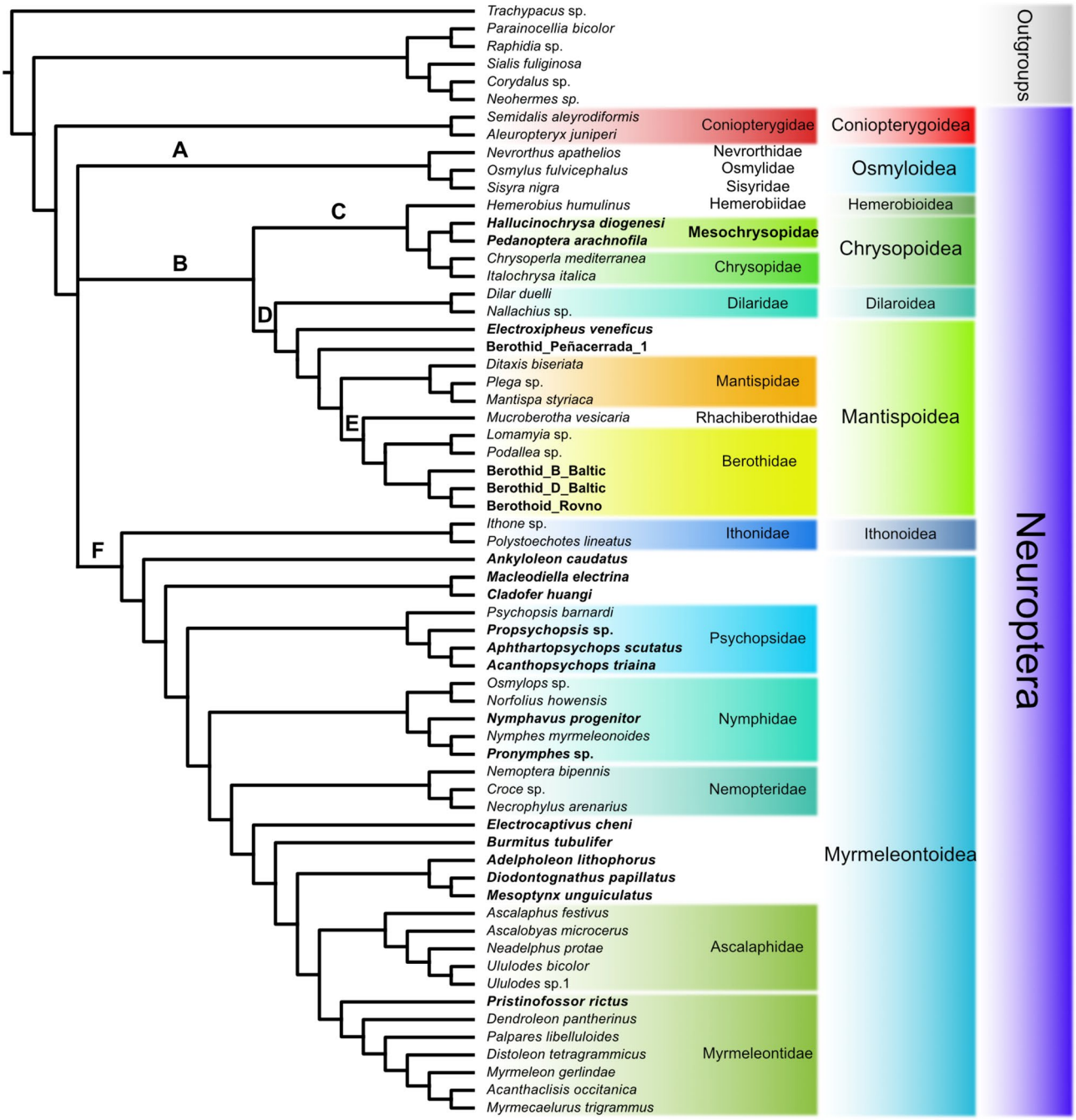

Figure 5. Phylogeny of Neuroptera based on larval morphology, including fossils, obtained under maximum parsimony. Strict consensus cladogram of two trees obtained under implied weights. Letters above branches indicate clades discussed in the text. Taxa in bold are fossils.

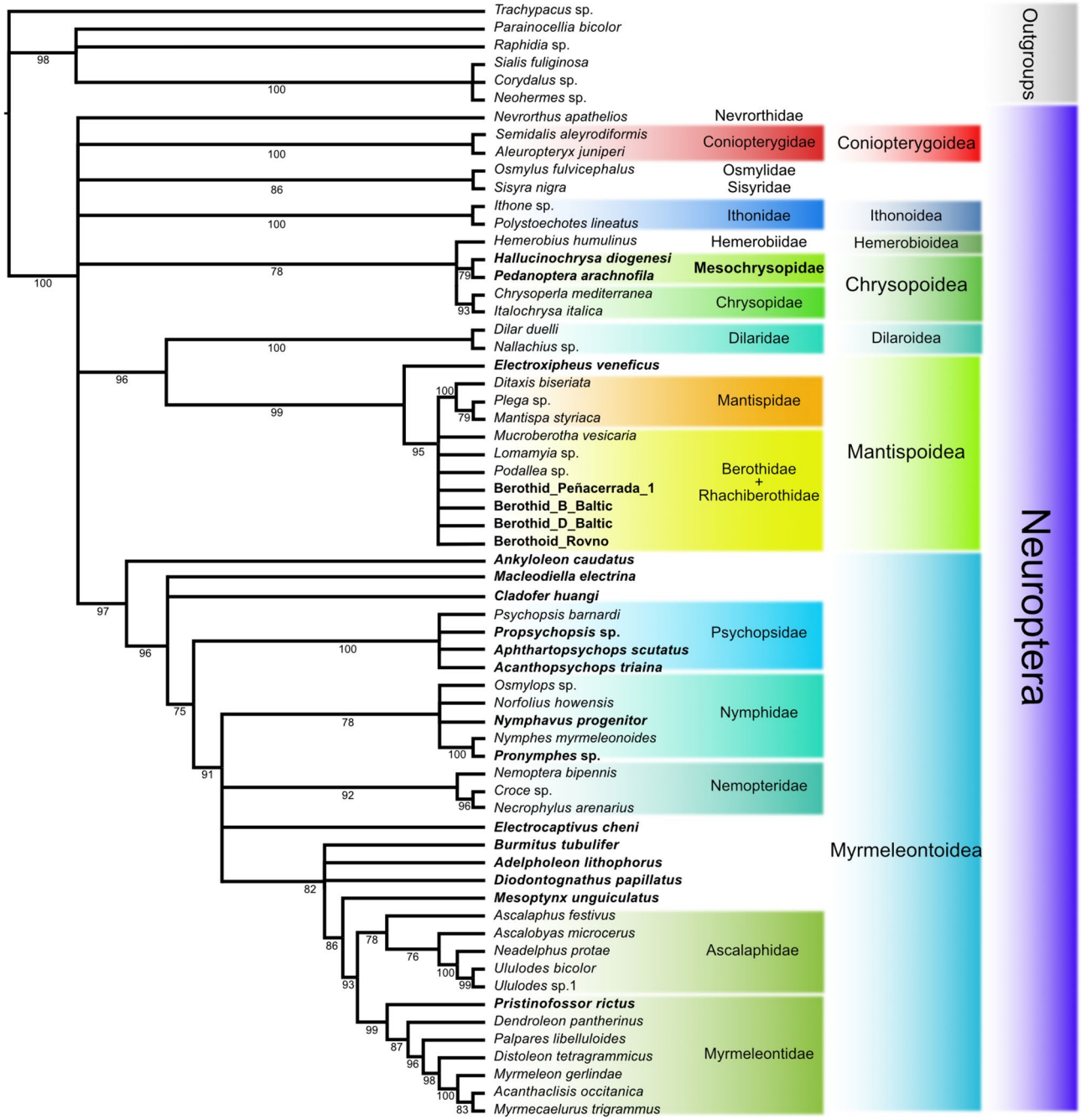

Figure 6. Phylogeny of Neuroptera based on larval morphology, including fossils, obtained under Bayesian inference. Numbers below branches are Bayesian posterior probabilities. Branches below 75 thresholds were collapsed. Taxa in bold are fossils.

lateral abdominal tendon present). Instead, under both EW and BI, the relationships among lacewings clades were not resolved. The IW search found three main subclades encompassing all the remaining lacewings: clade A (Osmyloidea), clade B and clade F (Ithonidae + Myrmeleontoidea). Monophyletic Osmyloidea were supported by one unique synapomorphy (73:1, posterior tentorial pits not in contact with subgenal ridge, ventro-lateral to it) and included Nevrorthidae as sister group to Osmylidae + Sisyridae. Osmyloidea were not recovered as monophyletic by both EW and BI, though both analyses recovered a poorly supported sister group relationship between Osmylidae and Sisyridae (MP Bremer support: 1; BI posterior probability: 86). MP analyses under both weighting schemes recovered clade B (MP Bremer support: 1), which encompassed two clusters: clade C, comprising Hemerobiidae as sister group to Chrysopoidea and clade D, including Dilaridae as sister group to Mantispoidea. Monophyly of Chrysopoidea, including living Chrysopidae and Mesozoic Mesochrysopidae, relied on one homoplasious synapomorphy (61:2) and obtained low supports (MP BS: 1), although both Chrysopidae (MP Bremer support: 1; BI posterior probabilities: 93) and Mesochrysopidae (MP Bremer support: 1; BI posterior

probability: 79) were recovered as monophyletic. Monophyly of the clade IV (Dilaridae + Mantispoidea) was supported by two unique synapomorphies (31:1, lateral remnants of frontoclypeal sulcus absent; 31:1, mandibulomaxillary stylets straight; 70:1, tentorial bridge reduced or absent) (MP Bremer support: 2; BI posterior probability: 96). Monophyly of Dilaridae relied on three unique (105:2, empodium stick-shaped; 107:1, pretarsal claws of prothoracic leg of different shape and size; 140:5, abdominal segment 10 with prominent paired cup-shaped adhesive pads) and three homoplasious synapomorphies and earned high supports (MP Bremer support: 4; BI posterior probability: 100). Mantispoidea, including *Electroxipheus*, were recovered as monophyletic based on one unique (104:1, unguitractor process present) and two homoplasious (20:2; 25:1) synapomorphies (MP Bremer support: 1; BI posterior probability: 96). *Electroxipheus* was consistently recovered as the sister group to all Mantispoidea in all analyses. The monophyly of the remaining Mantispoidea relied on one unique synapomorphy (3:1, head capsule > 1.5 times longer than wide). Under IW, the fossil specimen from Spanish amber MCNA9294 (Berothid_ Peñacerrada 1) was recovered as the sister group to all the remaining mantispoids, while monophyletic Mantispidae formed a dichotomy with a cluster (clade E) including Rhachiberothidae and living and fossil species of Berothidae. Instead, both EW and BI analyses found monophyletic Mantispidae emerging from a polytomy encompassing unresolved Berothidae and Rhachiberothidae. The monophyly of Mantispidae, which included *Plega* Navás (Symphrasinae) as sister group to *Mantispa* Illiger (Mantispinae) and *Ditaxis* McLachlan (Drepanicinae), relied on two homoplasious apomorphies (25:0; 40:4; 51:1), with high supports (MP Bremer support: 4; BI posterior probability: 100). Under IW, Clade E was supported by one unique (79:1, lateral sutures of head capsule present) and comprised extant representatives of Rhachiberothidae (*Mucroberotha*) and Berothidae (*Podallea* Navás, *Lomamyia* Banks) and several fossil larvae assigned to the berothids from Cenozoic ambers (Berothid_Baltic_B, Berothid_Baltic_D, Berothoid_Rovno). Under IW, Ithonidae clusterised with Myrmeleontiformia based on two unique (22:0, antennomere 3 with short sensilli; 79:1, head-thorax articulation dorsal) and one homoplasious (61:2) synapomorphies. The monophyly of Ithonidae was supported also under EW and BI with high supports supports (MP Bremer support: 10; BI posterior probability: 100), despite a sister group relationship to Myrmeleontiformia was not supported. Monophyly of Myrmeleontiformia, including living Myrmeleontoidea and their fossil relatives, was confirmed in all analyses (MP Bremer support: 1; BI posterior probability: 97).

Discussion

Phylogenetic signal and fossil placement

Larvae of holometabolous insects have been a main source of information for classification and phylogenetic studies[35], especially for Neuropterida[36]. Despite advances in genome- and transcriptome-based phylogenies, larvae remain crucial for understanding life histories, trait evolution tracing, and calibration points for divergence time estimation, as well as revealing ancient ecological networks. In this regard, *Electroxipheus* sheds new light on the morphology of fossil Neuroptera, enabling to reconstruct the evolutionary history of mantispoid lacewings. The results of the current phylogenetic analysis under IW diverge from other morphology-based reconstructions by identifying Coniopterygidae as sister group to all the other Neuroptera, Ithonidae as sister group to Myrmeleontoidea and supporting the monophyly of Osmyloidea (Fig. 5). These clades are also supported in phylogenetic analyses based on mitogenomes and transcriptomes[37–40]. However, the topology here retrieved was poorly resolved and the relationships obtained by enforcing IW were not corroborated under EW and BI (Fig. 6). Instead, in cladistic reconstructions, Nevrorthidae were recovered as sister group to all Neuroptera, not supporting the monophyly of Osmyloidea, while both Coniopterygidae and Ithonidae were part of a diverse clade encompassing all lineages characterised by a "maxillary-head" configuration" (i.e., the Hemerobiiformia)[7,8,28,41]. In agreement with previous cladistic reconstructions, the analyses recovered a sister group relationship between Hemerobiidae and Chrysopidae, and a clade encompassing Dilaridae and Mantispoidea, i.e., the "dilarid clade"[7,8,28,41,42]. However, molecular analyses consistently found Dilaridae as an isolated lineage and Hemerobiidae and Chrysopidae on different branches of the lacewing tree of life, though their phylogenetic affinities vary according to the dataset[37–40]. The discrepancies between morphology-based and molecular-based phylogenies in reconstructing the affinities of these lineages, suggests that the morphological larval traits supporting these relationships are likely homoplasious. The Mesozoic Mesochrysopidae are confirmed as sister group to living Chrysopidae, in agreement with the previous results[14]. Myrmeleontoidea emerge as a clade, in agreement with all phylogenetic studies[7,8,38,39] (Figs. 5, 6). The relationships between the lineages of Myrmeleontoidea and the placement of the fossil assigned to this clade agrees with the previous results of Badano et al.[14,15]. The monophyly of the lineages now included in Mantispoidea has long been recognized based on adult, larval and life-history characters and is supported in most phylogenetic analyses, although with major differences in morphology- and molecular-based reconstructions[7,24,28,38,43]. The present analyses consistently placed *Electroxipheus* as sister group to all the other mantispoids, finding it as a stem-group unrelated to any living lineage, as also implied by its unusual combination of morphological traits. The performed analyses supported the monophyly of Mantispidae including Symphrasinae, while the monophyly of Berothidae was only supported under IW. In contrast, cladistic analyses based on adult characters and molecular-based phylogenies retrieved Symphrasinae as sister group to either Rhachiberothidae or Berothidae[24,37,40]. The analyses confirmed that the fossil mantispoids included in the dataset belong to Mantispoidea but they were not confidently placed in any clade within the family. The largely unresolved Mantispoidea are likely affected by the inadequate state of knowledge of their immatures because most of the larvae of this clade, except for Mantispinae (Mantispidae), are still unknown. Our results suggest that our understanding of mantispoid larval diversity is still incomplete, hindering the reconstruction of the affinities of fossil larvae based on cladistic methods.

An unusual antenna

Drawing homologies between the segmentation of the antenna of the larvae of holometabolous insects and the main component of the antenna of the adult (i.e., scape, pedicel, flagellum) is notoriously challenging and the genetic pathway of the antenna subdivision is poorly understood[44]. The larval ground pattern of Neuroptera is characterised by an antenna with three main elements: a basal, an intermediate and an apical antennomere (Fig. 7). The presence of intrinsic musculature in the basal and of a vestigial Johnston organ in the intermediate antennomere in the first instar larva of *Dilar* Rambur suggest that they are homologous to the scape and the

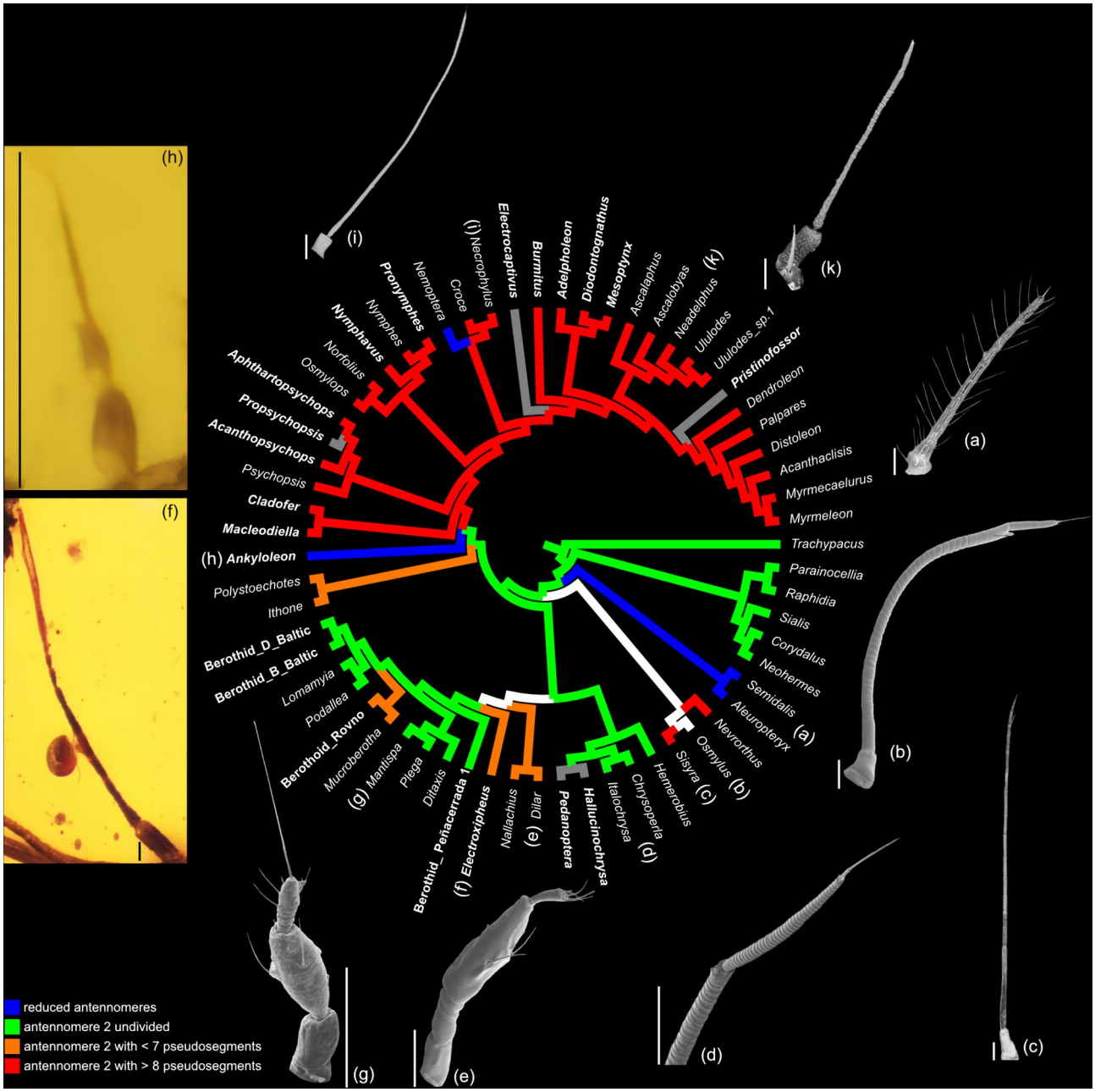

Figure 7. Morphological diversity of the shape and segmentation of the antennae of larval Neuroptera mapped on the maximum parsimony tree obtained under implied weights. Branch colors indicate the segmentation of the second antennomere. Genera in bold are fossils. (**a**) *Conwentzia psociformis* (Curtis) (Coniopterygidae); (**b**) *Osmylus fulvicephalus* (Scopoli) (Osmylidae); (**c**) *Sisyra nigra* (Retzius) (Sisyridae); (**d**) *Apertochrysa* sp. (Chrysopidae), detail of second and third antennomeres showing annulations; (**e**) *Dilar duelli* Aspöck and Aspöck (Dilaridae); (**f**) *Mantispa styriaca* (Poda), first instar (Mantispidae); (**g**) *Electroxipheus veneficus* gen. et sp. n., Burmite (stem-Mantispoidea); (**h**) *Ankyloleon caudatus* Badano, Haug and Cerretti, Burmite (stem-Myrmeleontiformia); (**i**) *Necrophylus arenarius* Roux (Nemopteridae); (**j**) *Puer maculatus* (Olivier) (Ascalaphidae). Scale bars: 40 µm. Photo courtesy by: (**a**) IRET-CNR SS (C. Cesaroni and R. A. Pantaleoni); (**b**–**j**) D. Badano.

pedicel, respectively[41]. The antenna is distinctly three segmented in several lineages of lacewings, such as: Osmylidae, most Mantispoidea (Berothidae, Mantispidae), Hemerobiidae and Chrysopidae (Fig. 7)[8,28,29]. Lacewing larvae with long antennae independently evolved adaptations to strengthen the second antennomere, which is usually the longest element. The larvae of Osmylidae are characterised by spiral sclerotization encircling and reinforcing the second element, while in Chrysopidae the second antennomere is annulated (Fig. 7)[29]. Instead, the antenna appears multisegmented in Nevrorthidae, Sisyridae, Dilaridae, Ithonidae and Myrmeleontoidea, because the second antennomere is followed by a series of short, often indistinct, irregular subsegments (Fig. 7)[8,29,30,42,45]. In the larvae of Dilaridae, the first instar larva has a distinctly three segmented antenna, while later instars are characterised by a subdivision of the second antennomere in subsegments through ring-shaped desclerotizations[41,45,46]. The segmentation pattern of the antenna of Dilaridae supports that the subsegments are not true antennomeres and are similar to the spirals and annulations of the antennae of Osmylidae and Chrysopidae. Conversely, the number of antennomeres is reduced in Coniopterygidae and Nemopteridae Nemopterinae (Fig. 7)[10,29,30]. Amber-embedded lacewing larvae from the Mesozoic show that a similar diversity in antennal shapes and segmentation patterns also characterised stem-lineages[15,47]. *Electroxipheus* differs from all the known larvae of Neuroptera in the segmentation of the antenna. In this specimen, the antenna consists of a robust basal antennomere (i.e., the scape), a long and thin second antennomere (i.e., the pedicel) followed by three short subsegments, and an apical antennomere with a short fusiform distal subsegment (Fig. 7). Therefore, the antenna of *Electroxipheus* differs from the three segmented antenna of most mantispoids. However, some poorly known fossil and living larvae of Rhachiberothidae and Berothidae are characterized by an apparently multisegmented antenna[33,34]. Yet, none of these larvae exhibit the unique antennal structure of the *Electroxipheus*. *Electroxipheus* shares with other lacewing lineages with superficially multisegmented antenna (e.g., Sisyridae and Myrmeleontoidea) a long second antennomere, suggesting that the article-like subsegments originate from divisions of an ancestrally three segmented antenna.

Piercing, venom delivery and sucking system

The main apomorphy of Neuroptera is represented by the transformation of the larval mouthparts in a complex suction apparatus[48]. The present fossil larva offers unique insights into the functional morphology of the envenomation and sucking system of a Mesozoic stem-lineage of lacewings. The shape of the mouthparts of *Electroxipheus* closely resembles the structure of piercing straight stylets characterising the larvae of Dilaridae and Mantispoidea (except for the curved-jawed larvae of Symphrasinae)[27,29]. However, *Electroxipheus* stands apart from the latter families because the mouthparts are proportionally longer and slightly curved outward and bent downward, while in most extant Mantispoidea the stylets are usually short and straight[28,29]. The maxillary stylet of *Electroxipheus* is thicker than the mandible, like all Neuroptera except for Myrmeleontoidea. The interlocking system between the mandible and the maxilla is well preserved and is similar to living species, consisting of a ventral guide on mandible and a corresponding rail on dorsal side of maxillary stylet (Fig. 4)[49]. In the apical-most section of the mouthparts, the suction channel of the fossil larva narrows and shifts dorsally, until it is almost completely encased by the mandible. A similar condition is present in the larvae of *Osmylus* Latreille near the channel opening at the mandible apex[50]. The poison channel is also distinct, running for the entire length of the maxillary stylet. In the apical section of the stylet, the poison channel migrates dorsally but remains separated from the suction channel by the walls of the maxillary stylet (Fig. 4). The mouthpart structure of *Electroxipheus* is largely congruent with that of living species, suggesting that the anatomy of the sucking and venom delivery system is strongly conservative across Neuroptera for their whole evolutionary history.

Palaeobiology

Among Neuroptera, the life histories of Mantispoidea are arguably the most remarkable, showing unusual morphologies, bizarre developmental strategies, and peculiar specializations to highly specific prey. However, at the same time, their larvae are probably the less known among lacewings and life history and morphological data are available for a handful of species, except for Mantispidae Mantispinae[33]. All the known Mantispoidea are characterized by physogastric later larval instars, a feature also documented in Burmese amber[23]. All the living genera of Berothidae with known later larval instars (i.e., *Isoscelipteron* Costa, *Lomamyia* and *Podallea*) have termitophilous larvae living in termite nests, of which the second and the third instars are physogastric. The second instar is also immobile and does not feed[33,51]. Mantispinae and Symphrasinae exhibit more drastic ontogenetic changes between instars than berothids and the development is hypermetamorphic, with deep changes in the anatomy of the head and of the appendages[7,29]. The larvae of Mantispidae Mantispinae feed on spider eggs within the egg sacs and according to the species can directly penetrate the egg sac or board the spider waiting for the sac production to enter in it[52,53]. Instead, Symphrasinae (i.e., *Anchieta* Navás and *Plega*) feed on pupae of holometabolans and most species were obtained from nests of eusocial hymenopterans[27]. However, the lack of data on the life history of most species of Berothidae, Rhachiberothidae and the other subfamilies of

Mantispidae, impairs our understanding of the development strategies and larval diversity of the clade. Larvae of Mantispoidea are known in both Mesozoic and Cenozoic ambers and appear particularly well represented in Burmese amber[21,33,34,54,55]. The inclusion of *Electroxipheus* in a phylogenetic context, coupled with high resolution XPCT imaging, allows us to place this specimen in the mantispoid phylogenetic tree and trace the evolution of life history and morphological traits across the lineage. The stem-group position of *Electroxipheus* offers valuable insights into the development of the unusual life strategies of Mantispoidea. Despite the challenge in ascertaining the instar of *Electroxipheus*, its body proportions suggest that it likely belongs to a non-physogastric second or third instar. The presence of short head capsule, long and thin antenna, long mandibulo-maxillary stylet and strongly developed basal maxillary elements indicate that *Electroxipheus* was an active predator. A predatory lifestyle is also suggested by comparisons with the larvae of unrelated lacewing lineages of active predators, such as Osmylidae, Chrysopidae and Hemerobiidae, to which it resembles in body proportions. The larva exhibits a remarkable convergence with the larvae of Osmylidae, both sharing elongated and curved outward mandibulo-maxillary stylets, although this feature is less prominent in *Electroxipheus* than in osmylids. Despite *Electroxipheus* shared its palaeoenvironment with a remarkable diversity of mantispoid larvae[21], its phylogenetic position and functional morphology suggest it belongs to a lineage that diverged from other mantispoids before the evolution of the physogastric development strategy.

Materials and methods

Data matrix

The dataset of morphological trait was compiled by implementing and updating the matrix originally developed by Badano et al.[15,30] using Mesquite v.3.61 software[56]. In turn, the dataset draws from the examination of both specimens and relevant literature, with a focus on comparative and cladistic studies[8–10,28,29,41,42,50]. The updated dataset comprises 63 taxa, including four extinct taxa from Mesozoic and Cenozoic amber deposits, as well as two extant ones (Table 1). The final version of the dataset included 63 taxa and 142 characters, consisting of 109 binary and 33 multistate (Supplementary Information File S1). The morphological details of fossil taxa were obtained from literature (Table 1), while direct observations were used for the new larva. Classification system follows Winterton et al. [38].

Phylogenetic analyses

Maximum parsimony (MP) analyses of the dataset were performed using the TNT v1.5 software[57] under both equal (EW) and implied (IW) weights. Heuristic tree explorations were conducted by setting the "traditional search option" under the following configurations: general RAM of 1000 Mbytes, memory se to hold 1 000 000 trees, 1000 replicates with tree bisection-reconnection (TBR) branch swapping and keeping 1000 trees per replicate. Under IW, the dataset was analyzed enforcing a wide spectrum of concavity k-values of the weighting function, from k = 3 to k = 20, while the most suitable one was found through the TNT script "setk.run"[58]. Multistate characters were considered as unordered and zero-length branches were collapsed. Bremer support values under EW were computed in TNT from 10 000 trees up to ten steps longer than the shortest trees obtained under the "traditional search", using the "trees from RAM" setting. Character state changes were plotted with WinClada v.1.00.08[59]. Consistency (CI) and retention (RI) indexes for matrix were calculated with Mesquite v.3.61 software. Ancestral State Reconstruction for character changes were perfomed with Mesquite v.3.61, with the likelihood ancestral state.

Bayesian inference (BI) analyses were run in MrBayes v.3.2.7 on the Extreme Science and Engineering Discovery Environment at Cyberinfrastructure for Phylogenetic Research[60]. The analyses were performed under the Mk1 model[61] with scoring set for variable morphological characters. Four Markov chain Monte Carlo (MCMC) chains, of which one cold and three heated, were run for 10^6 generations, setting a burn-in fraction of 50% and sampling the chains every 1000 generations. The convergence of independent runs was assessed through the average standard deviation of split frequencies (< 0.01) and potential scale reduction factors (approaching 1). Ancestral state reconstructions for characters 'Antennomere 2 segmentation' (17) was carried out in Mesquite 3.61[56] using maximum likelihood and plotted on the strict consensus IW tree.

Optical examination

Specimens were examined, photographed, and measured with a Zeiss Axio Zoom. V16 stereoscope.

Original specimen code or name	Type locality and age	Occurence	Classification	Reference	Name used in present dataset
MCNA9294	Peñacerrada 1, Basque-Cantabrian Basin	Cretaceous, late Albian: Spain	Berothidae	Pérez-de la Fuente et al.[55]	Berothid_ Peñacerrada 1
Berothid indet., larva B	Baltic amber	Eocene	Berothidae	Wedmann et al.[33]	Berothid_Baltic_B
Berothid indet., larva D	Baltic amber	Eocene	Berothidae	Wedmann et al.[33]	Berothid_Baltic_D
Berothoid	Rovno amber, Klesov deposit, Sarny district, Rovno Region, Ukraine	Late Eocene	Mantispoidea indet	Makarkin et al.[34]	Berothoid_Rovno

Table 1. Additional fossil larvae of Mantispoidea included in the phylogenetic analysis.

XPCT measurements

The experiments were carried out at the TOMCAT beamline of the Swiss Light Source (Villigen, Switzerland). The incident monochromatic X-ray energy was of 20 keV. A PCO edge 5.5 camera coupled with optics resulting in a pixel size of $1.625 \times 1.625\,\mu m^2$ and $0.32 \times 0.32\,\mu m^2$ was set at a distance from the sample of 3 (exposure time = 90 ms) and 5 cm (exposure time = 220 ms), respectively. The tomographic images were acquired using the so-called half-acquisition mode, which allows to almost double the image field of view.

Data pre-processing, phase retrieval, and reconstruction (by using Filtered Back Projection (FBP) method) were performed on site using by means of ad hoc software based on the Paganin's phase retrieval algorithm. Image processing and 3D rendering were made with the software ImageJ (https://imagej.net/Fiji) and VG studioMax. The different electron densities of the tissues were rendered as grey levels in the phase tomograms images. For the 3D rendering, binarization was further applied over the reconstructed data.

Data availability

The data that supports the findings of this study are available in the supporting information of this article.Supplementary Movie S1.Supplementary Figures.Supplementary Information.

Received: 26 April 2024; Accepted: 9 August 2024
Published online: 24 August 2024

References

1. Walker, A. A. *et al.* Entomo-venomics: The evolution, biology and biochemistry of insect venoms. *Toxicon* **154**, 15–27 (2018).
2. Fry, B. G. *et al.* The toxicogenomic multiverse: Convergent recruitment of proteins into animal venoms. *Annu. Rev. Genomics Hum. Genet.* **10**, 483–511 (2009).
3. Schmidt, J. O. Biochemistry of insect venoms. *Annu. Rev. Entomol.* **27**, 339–368 (1982).
4. Misof, B. *et al.* Phylogenomics resolves the timing and pattern of insect evolution. *Science* **346**, 763–767 (2014).
5. Engel, M. S., Winterton, S. L. & Breitkreuz, L. C. V. Phylogeny and Evolution of Neuropterida: Where Have Wings of Lace Taken Us?. *Annu. Rev. Entomol.* **63**, 531–551 (2018).
6. Oswald, J. D. & Machado, R. J. P. Biodiversity of the Neuropterida (Insecta: Neuroptera, Megaloptera, and Raphidioptera). In *Insect Biodiversity Science and Society* (ed. Foottit, R. G.) (Wiley, 2018).
7. Aspöck, U., Plant, J. D. & Nemeschkal, H. L. Cladistic analysis of Neuroptera and their systematic position within Neuropterida (Insecta: Holometabola: Neuropterida: Neuroptera). *Syst. Entomol.* **26**, 73–86 (2001).
8. Beutel, R. G., Friedrich, F. & Aspöck, U. The larval head of Nevrorthidae and the phylogeny of Neuroptera (Insecta). *Zool. J. Linn. Soc.* **158**, 533–562 (2010).
9. Wundt, H. Der Kopf der Larve von *Osmylus chrysops* L. (Neuroptera, Planipennia). *Jb. Anat.* **662**, 557–662 (1961).
10. Rousset, A. Morphologie céphalique des larves de planipennes (Insectes Névroptéroïdes). *Mém. Mus. natl. hist. nat.* **42**, 1–199 (1966).
11. Zimmermann, D., Randolf, S. & Aspöck, U. From Chewing to Sucking via Phylogeny—From Sucking to Chewing via Ontogeny: Mouthparts of Neuroptera. In *Insect Mouthparts: Form, Function, Development and Performance* (ed. Krenn, H. W.) (Springer, 2019).
12. Matsuda, K. *et al.* Purification and Characterization of a Paralytic Polypeptide from Larvae of *Myrmeleon bore*. *Biochem. Biophys. Res. Commun.* **215**, 167–171 (1995).
13. Pérez-de La Fuente, R. *et al.* Early evolution and ecology of camouflage in insects. *Proc. Natl. Acad. Sci. USA* **109**, 21414–21419 (2012).
14. Badano, D., Engel, M. S., Basso, A., Wang, B. & Cerretti, P. Diverse Cretaceous larvae reveal the evolutionary and behavioural history of antlions and lacewings. *Nat. Commun.* **9**, 3257. https://doi.org/10.1038/s41467-018-05484-y (2018).
15. Badano, D. *et al.* X-ray microtomography and phylogenomics provide insights into the morphology and evolution of an enigmatic Mesozoic insect larva. *Syst. Entomol.* **46**, 672–684 (2021).
16. Haug, C., Braig, F. & Haug, J. T. Quantitative analysis of lacewing larvae over more than 100 million years reveals a complex pattern of loss of morphological diversity. *Sci. Rep.* **13**, 6127. https://doi.org/10.1038/s41598-023-32103-8 (2023).
17. Shi, G. *et al.* Age constraint on Burmese amber based on U-Pb dating of zircons. *Cretac. Res.* **37**, 155–163 (2012).
18. Wang, B. *et al.* Debris-carrying camouflage among diverse lineages of Cretaceous insects. *Sci. Adv.* **2**, e1501918. https://doi.org/10.1126/sciadv.1501918 (2016).
19. Liu, X., Zhang, W., Winterton, S. L., Breitkreuz, L. C. V. & Engel, M. S. Early Morphological Specialization for Insect-Spider Associations in Mesozoic Lacewings. *Curr. Biol.* **26**, 1590–1594 (2016).
20. Liu, X. *et al.* Liverwort Mimesis in a Cretaceous Lacewing Larva. *Curr. Biol.* **28**, 1475–1481 (2018).
21. Haug, J. T. *et al.* Changes in the morphological diversity of larvae of lance lacewings, mantis lacewings and their closer relatives over 100 million years. *Insects* **12**, 860. https://doi.org/10.3390/insects12100860 (2021).
22. Lu, X. & Liu, X. The Neuropterida from the mid-Cretaceous of Myanmar: A spectacular palaeodiversity bridging the Mesozoic and present faunas. *Cretac. Res.* **121**, 104727. https://doi.org/10.1016/j.cretres.2020.104727 (2021).
23. Haug, J. T. & Haug, C. 100 Million-year-old straight-jawed lacewing larvae with enormously inflated trunks represent the oldest cases of extreme physogastry in insects. *Sci. Rep.* **12**, 12760. https://doi.org/10.1038/s41598-022-16698-y (2022).
24. Ardila-Camacho, A., Califre Martins, C., Aspöck, U. & Contreras-Ramos, A. Comparative morphology of extant raptorial Mantispoidea (Neuroptera: Mantispidae, Rhachiberothidae) suggests a non-monophyletic Mantispidae and a single origin of the raptorial condition within the superfamily. *Zootaxa* **4992**, 1–89 (2021).
25. Tafforeau, P. *et al.* Applications of X-ray synchrotron microtomography for non-destructive 3D studies of paleontological specimens. *Appl. Phys. A. Mater. Sci. Process.* **83**, 195–202 (2006).
26. Lak, M. *et al.* Phase contrast X-ray synchrotron imaging: Opening access to fossil inclusions in opaque amber. *Microsc. Microanal.* **14**, 251–259 (2008).
27. Ardila-Camacho, A., Pires Machado, R. J. & Contreras-Ramos, A. A review of the biology of Symphrasinae (Neuroptera: Rhachiberothidae), with the description of the egg and primary larva of *Plega* Navás, 1928. *Zool. Anz.* **294**, 165–185 (2021).
28. Jandausch, K., Pohl, H., Aspöck, U., Winterton, S. L. & Beutel, R. G. Morphology of the primary larva of *Mantispa aphavexelte* Aspöck & Aspöck, 1994 (Neuroptera: Mantispidae) and phylogenetic implications to the order of Neuroptera. *Arthropod. Syst. Phyl.* **76**, 529–560 (2018).
29. MacLeod, E. G. A comparative morphological study of the head capsule and cervix of larval Neuroptera (Insecta). PhD thesis (Harvard University, London). (1964).
30. Badano, D., Aspöck, U., Aspöck, H. & Cerretti, P. Phylogeny of Myrmeleontiformia based on larval morphology (Neuropterida: Neuroptera). *Syst. Entomol.* **42**, 94–117 (2017).

31. Minter, L. R. A comparison of the eggs and first-instar larvae of *Mucroberotha vesicaria* Tjeder with those of other species in the families Berothidae and Mantispidae (Insecta: Neuroptera). *Advances in Neuropterology. Proceedings of the Third International Symposium on Neuropterology* (eds. Mansell, M. W. & Aspöck, H.) 115–129 (1990).
32. Dorey, J. B. & Merritt, D. J. First observations on the life cycle and mass eclosion events in a mantis fly (Family Mantispidae) in the subfamily Drepanicinae. *Biodivers. Data. J.* **5**, e21206. https://doi.org/10.3897/BDJ.5.e21206 (2017).
33. Wedmann, S., Makarkin, V. N., Weiterschan, T. & Hörnschemeyer, T. First fossil larvae of Berothidae (Neuroptera) from Baltic amber, with notes on the biology and termitophily of the family. *Zootaxa* **3716**, 236–258 (2013).
34. Makarkin, V. N. & Perkovsky, E. E. A remarkable fossil berothoid larva (Neuroptera) from the late Eocene Rovno amber (Ukraine). *Hist. Biol.* https://doi.org/10.1080/08912963.2023.2297909 (2024).
35. Meier, R. & Lim, G. S. Conflict, convergent evolution, and the relative importance of immature and adult characters in endopterygote phylogenetics. *Annu. Rev. Entomol.* **54**, 85–104 (2009).
36. Engel, M. S., Winterton, S. L. & Breitkreuz, L. C. V. Phylogeny and Evolution of Neuropterida: Where Have Wings of Lace Taken Us?. *Annu. Rev. Entomol.* **63**, 531–551 (2017).
37. Wang, Y. *et al.* Mitochondrial phylogenomics illuminates the evolutionary history of Neuropterida. *Cladistics* **33**, 617–636 (2017).
38. Winterton, S. L. *et al.* Evolution of lacewings and allied orders using anchored phylogenomics (Neuroptera, Megaloptera, Raphidioptera). *Syst. Entomol.* **43**, 330–354 (2018).
39. Vasilikopoulos, A. *et al.* An integrative phylogenomic approach to elucidate the evolutionary history and divergence times of Neuropterida (Insecta: Holometabola). *BMC Evol. Biol.* **20**, 64. https://doi.org/10.1186/s12862-020-01631-6 (2020).
40. Cai, C., Tihelka, E., Liu, X. & Engel, M. S. Improved modelling of compositional heterogeneity reconciles phylogenomic conflicts among lacewings. *Palaeoentomology* **6**, 49–57 (2023).
41. Li, D. *et al.* Cephalic anatomy highlights morphological adaptation to underground habitats in a minute lacewing larva of *Dilar* (Dilaridae) and conflicting phylogenetic signal in Neuroptera. *Insect Sci.* **30**, 1445–1463 (2023).
42. Li, D. *et al.* Unearthing underground predators: The head morphology of larvae of the moth lacewing genus *Ithone* Newman (Neuroptera: Ithonidae) and its functional and phylogenetic implications. *Syst. Entomol.* **47**, 618–636 (2022).
43. Winterton, S. L., Hardy, N. B. & Wiegmann, B. M. On wings of lace: Phylogeny and Bayesian divergence time estimates of Neuropterida (Insecta) based on morphological and molecular data. *Syst. Entomol.* **35**, 349–378 (2010).
44. Minelli, A. The insect antenna: Segmentation, patterning and positional homology. *J. Entomol. Acarol. Res.* **49**, 59–66 (2017).
45. Ghilarov, M. S. The larva of *Dilar turcicus* Hag. and the position of the family Dilaridae in the suborder Planipennia. *Entomol. Rev.* **41**, 244–253 (1962).
46. Badano, D., Di Giulio, A., Aspöck, H., Aspöck, U. & Cerretti, P. Burrowing specializations in a lacewing larva (Neuroptera: Dilaridae). *Zool. Anz.* **293**, 247–256 (2021).
47. Haug, J. T., Baranov, V., Müller, P. & Haug, C. New extreme morphologies as exemplified by 100 million-year-old lacewing larvae. *Sci. Rep.* **11**, 20432. https://doi.org/10.1038/s41598-021-99480-w (2021).
48. Aspöck, U., Haring, E. & Aspöck, H. The Phylogeny of the Neuropterida: Long Lasting and Current Controversies and Challenges (Insecta: Endopterygota). *Arthropod. Syst. Phyl.* **70**, 119–129 (2012).
49. Gaumont, J. L'appareil digestif des larves de Planipennes. *Ann. Sci. Nat Zool. Biol. Anim.* **18**, 145–250 (1976).
50. Jandausch, K., Beutel, R. G. & Bellstedt, R. The larval morphology of the spongefly *Sisyra nigra* (Retzius, 1783) (Neuroptera: Sisyridae). *J. Morphol.* **280**, 1742–1758 (2019).
51. Möller, A., Minter, L. R. & Olivier, P. A. S. Larval morphology of *Podallea vasseana* Navás and *Podallea manselli* Aspöck & Aspöck from South Africa (Neuroptera: Berothidae). *Afr. Entomol.* **14**, 1–12 (2006).
52. Redborg, K. E. Biology of the Mantispidae. *Annu. Rev. Entomol.* **43**, 175–194 (1998).
53. Haug, J. T., Müller, P. & Haug, C. The ride of the parasite: A 100-million-year old mantis lacewing larva captured while mounting its spider host. *Zool. Lett.* https://doi.org/10.1186/s40851-018-0116-9 (2018).
54. Engel, M. S. & Grimaldi, D. A. Diverse Neuropterida in Cretaceous amber, with particular reference to the paleofauna of Myanmar (Insecta). *Nova Suppl. Entomol.* **20**, 1–86 (2008).
55. Pérez-de la Fuente, R., Engel, M. S., Delclòs, X. & Peñalver, E. Straight-jawed lacewing larvae (Neuroptera) from Lower Cretaceous Spanish amber, with an account on the known amber diversity of neuropterid immatures. *Cretac. Res.* https://doi.org/10.1016/j.cretres.2019.104200 (2020).
56. Maddison, W. P. & Maddison, D. R. Mesquite: A Modular System for Evolutionary Analysis. http://mesquiteproject.org (2021).
57. Goloboff, P. A. & Catalano, S. A. TNT version 15, including a full implementation of phylogenetic morphometrics. *Cladistics* **32**, 221–238 (2016).
58. Santos, B. F., Payne, A., Pickett, K. M. & Carpenter, J. M. Phylogeny and historical biogeography of the paper wasp genus *Polistes* (Hymenoptera: Vespidae): Implications for the overwintering hypothesis of social evolution. *Cladistics* **31**, 535–549 (2015).
59. Nixon, K. C. WinClada. version 1.00.08 (Available at http://www.cladistics.com, 2002).
60. Miller, M. A., Pfeiffer, W. T. & Schwartz, T. Creating the CIPRES Science Gateway for inference of large phylogenetic trees. In *Proceedings of the Gateway Computing Environments Workshop (GCE)* (ed. Schwartz, T.) (IEEE, 2010).
61. Lewis, P. O. A likelihood approach to estimating phylogeny from discrete morphological character data. *Syst. Biol.* **50**, 913–925 (2001).

Acknowledgements

This work received support from the European Union–NextGenerationEU as part of the National Biodiversity Future Center, Italian National Recovery and Resilience Plan (NRRP) Mission 4 Component 2 Investment 1.4 (CUP: B83C22002950007 [Sapienza]; B63C22000650007 [Siena]). We thank the Willi Hennig Society for making the TNT software available. Special thanks to Roberto A. Pantaleoni (IRET CNR SS, Italy) for sharing and letting us use the photo of coniopterygid antenna. We acknowledge the Paul Scherrer Institut, Villigen, Switzerland, for provision of synchrotron radiation beamtime at the TOMCAT beamline X02DA of the Swiss Light Source and would like to thank Margie Olbinado and the whole staff of the beamline for assistance. We thank the referees for the critical review of the manuscript.

Author contributions

D.B. and P.C. conceived and designed the experiments. D.B. studied and described the material. M.F., L.M., F.P. and N.P. performed the experiment using XPCT and designed digital reconstructions and animations. D.B. analyzed the data. D.B., P.C. and M.F. wrote the main manuscript. All authors reviewed the manuscript.

Competing interests

The authors declare no competing interests.

Additional information

Supplementary Information The online version contains supplementary material available at https://doi.org/10.1038/s41598-024-69887-2.

Correspondence and requests for materials should be addressed to D.B.

Reprints and permissions information is available at www.nature.com/reprints.

Publisher's note Springer Nature remains neutral with regard to jurisdictional claims in published maps and institutional affiliations.